

Supporting Information

**3D Crinkled MXene/TiO<sub>2</sub> Heterostructure with Interfacial Coupling for Ultra-Fast and Reversible Potassium Storage**

Xinyue Zhang <sup>a</sup>, Jing Wang <sup>a</sup>, Yuting Jiang <sup>a</sup>, Meng Zhang <sup>a</sup>, Huihua Min <sup>b</sup>, Hao Yang <sup>\*,a</sup>, Jin Wang <sup>\*,a</sup>

<sup>a</sup> College of Materials Science and Engineering, Nanjing Tech University, Nanjing 211800, PR China

<sup>b</sup> Electron Microscope Lab, Nanjing Forestry University, Nanjing 210037, Jiangsu, PR China

**Corresponding Author**

\* E-mail: mse\_yanghao@njtech.edu.cn (Hao Yang); msejwang@njtech.edu.cn (Jin Wang)

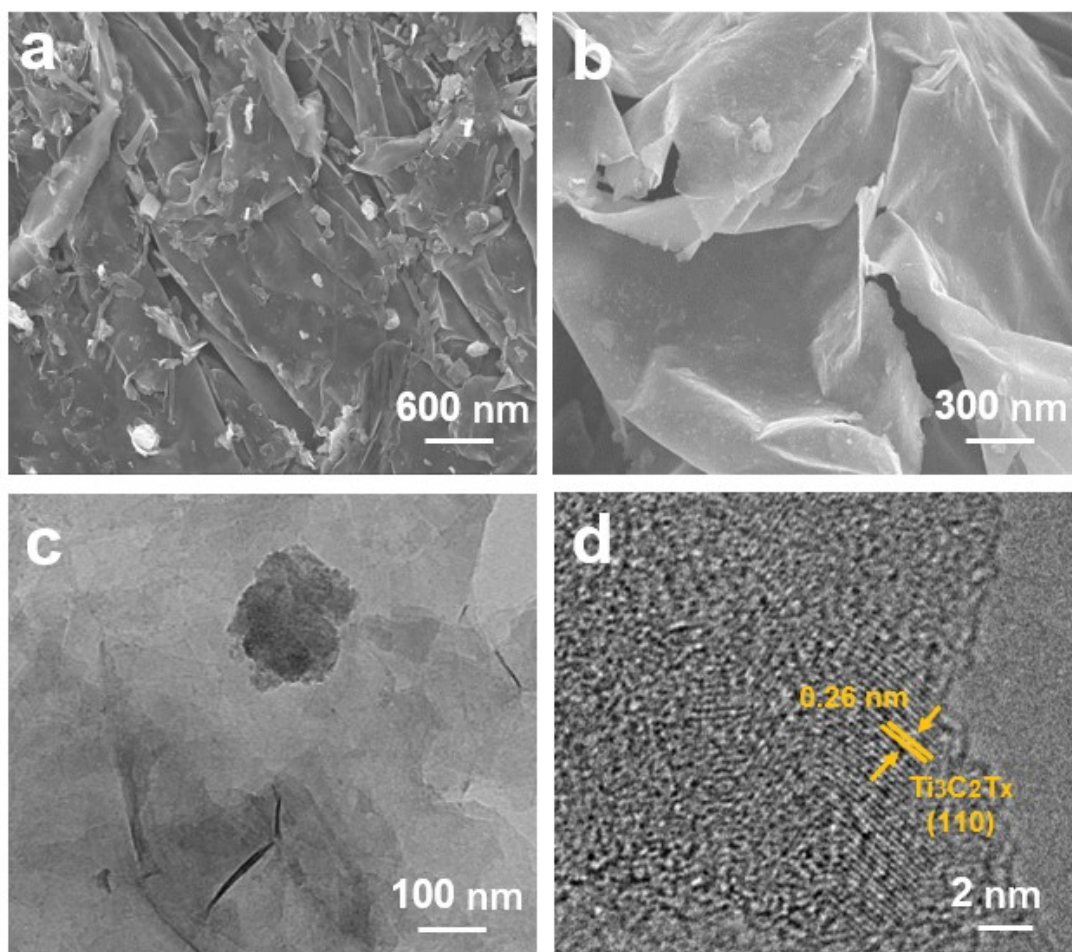


**Figure S1** (a)-(b) SEM images, (c) TEM image and (d) HRTEM image of MXene.

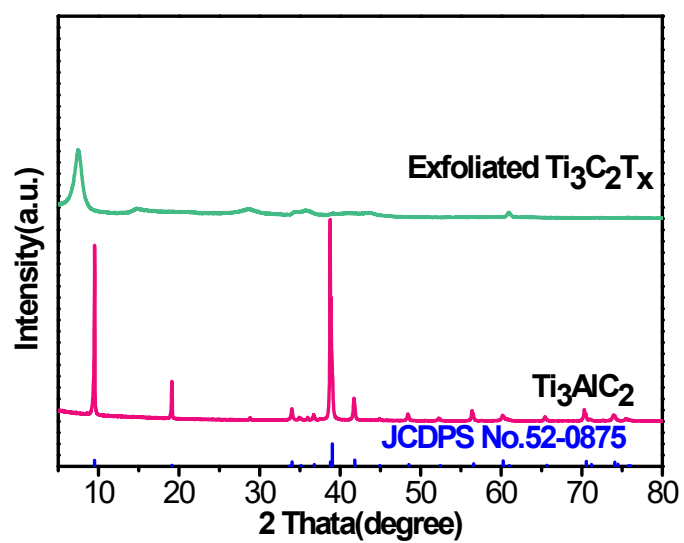
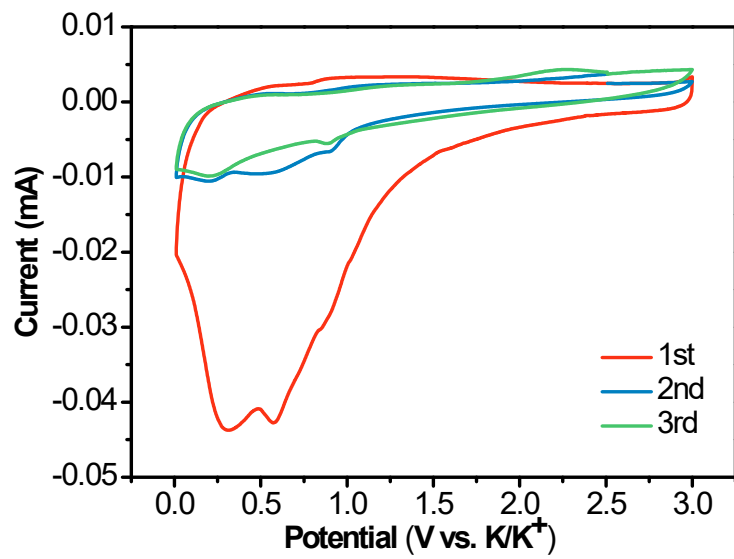
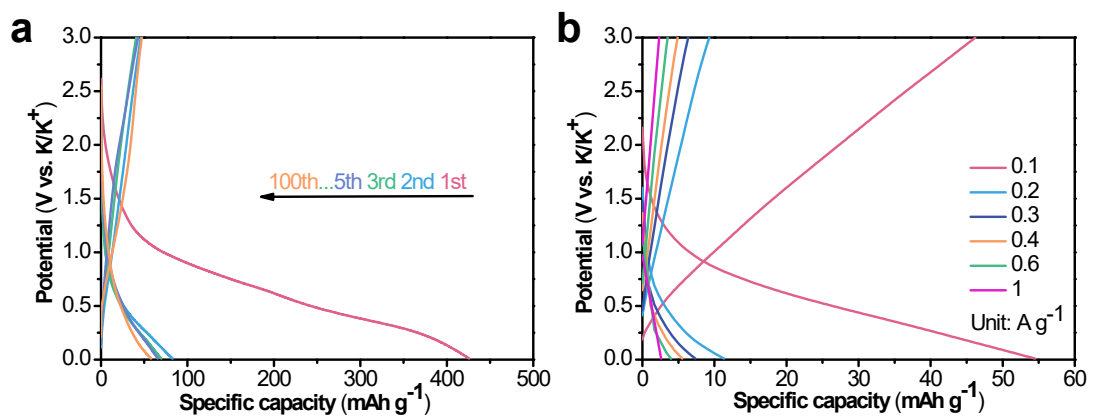


Figure S2 XRD patterns of  $Ti_3AlC_2$  and  $Ti_3C_2T_x$  nanosheets.



**Figure S3** CV curves of CM at a scan rate of 0.1 mV s<sup>-1</sup>.



**Figure S4** (a) Galvanostatic charge/discharge curves of CM at  $0.05 \text{ A g}^{-1}$ . (b) The charge/discharge profiles of CM at different current densities.

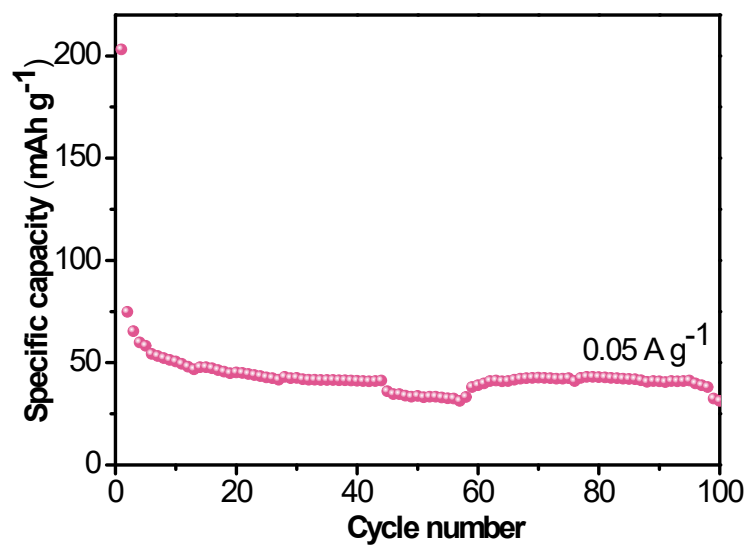


**Figure S5** Cycle performance of MXene at  $0.05 \text{ A g}^{-1}$  over 100 cycles.

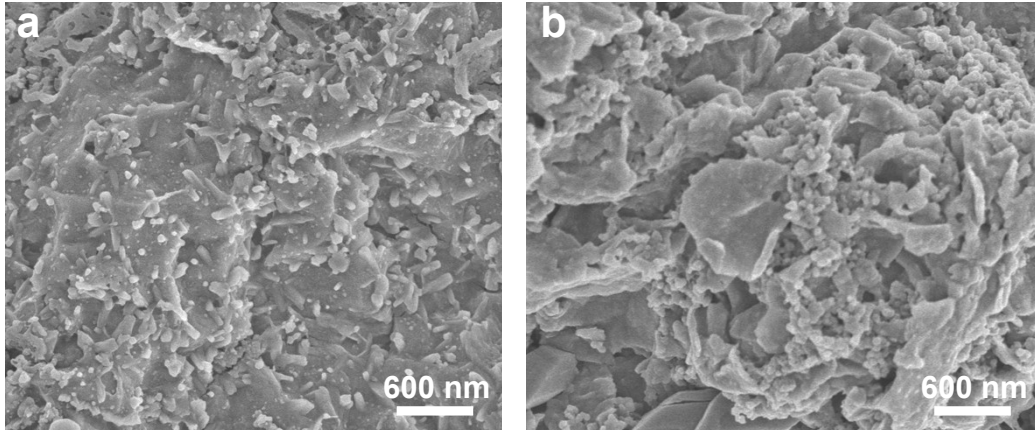


**Figure S6** (a) SEM images of CM/TiO<sub>2</sub> after cycle at 0.05 A g<sup>-1</sup>. (b) SEM images of CM after cycle at 0.05 A g<sup>-1</sup>.

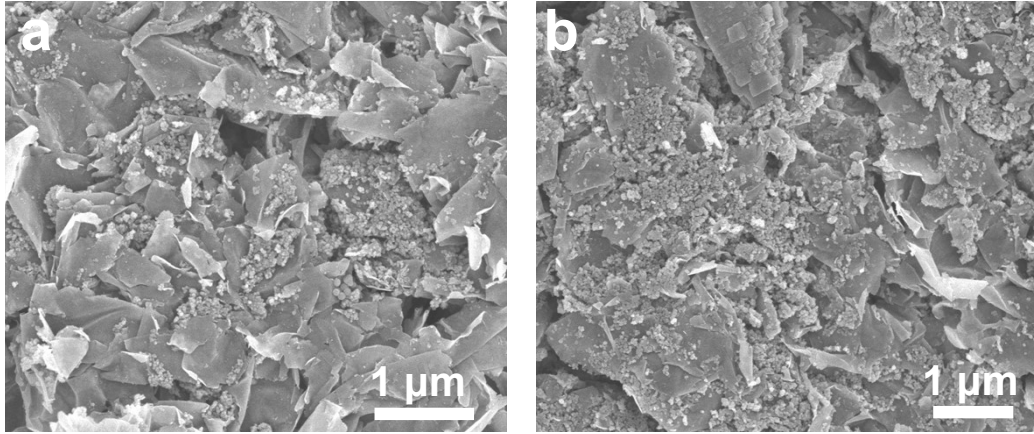


**Figure S7** (a) SEM images of CM/TiO<sub>2</sub>-3h. (b) SEM images of CM/TiO<sub>2</sub>-4h.



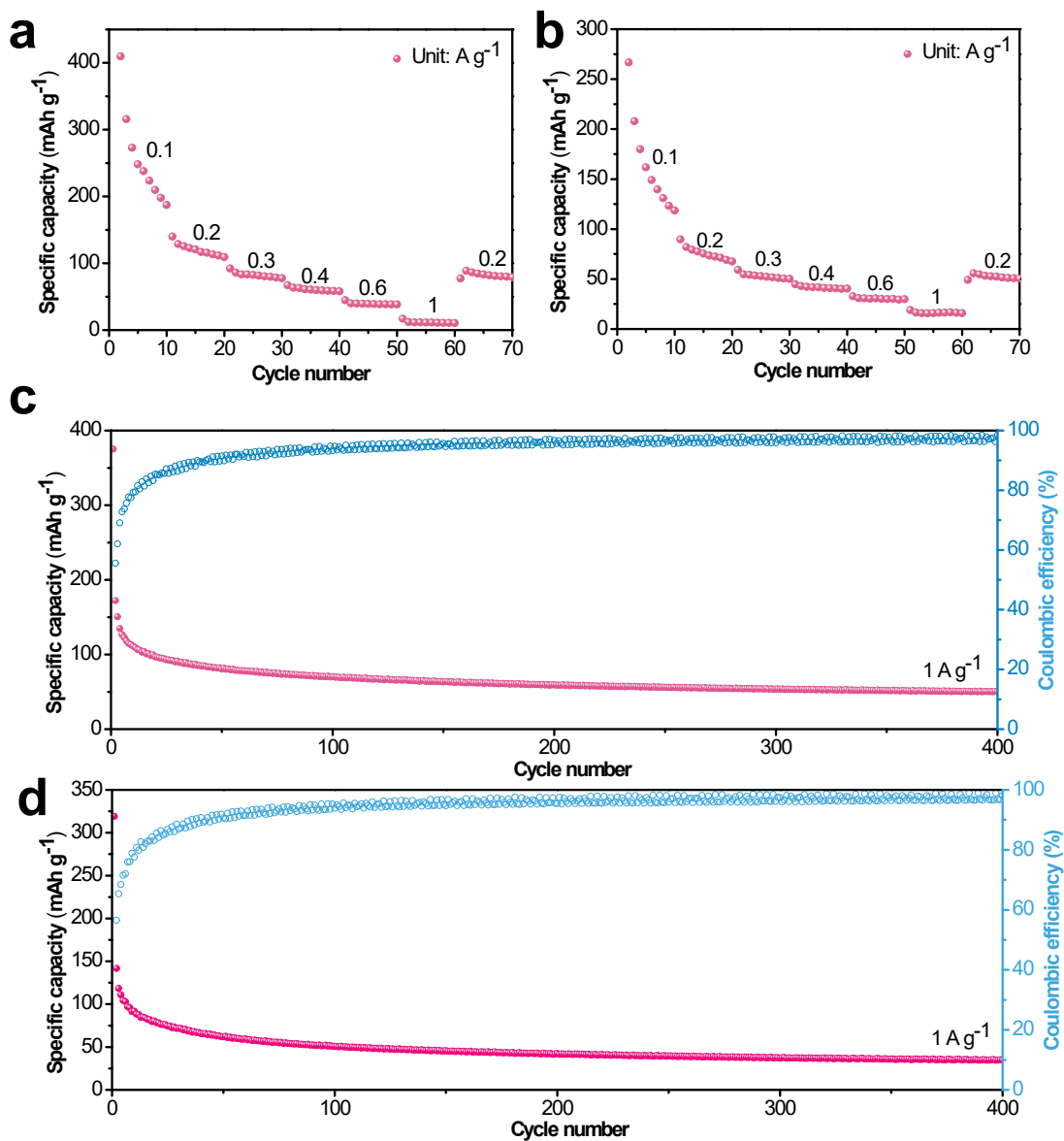


**Figure S8** (a) Rate capability of CM/TiO<sub>2</sub>-3h at various current densities. (b) Rate capability of CM/TiO<sub>2</sub>-4h at various current densities. (c) Long cycle performance of CM/TiO<sub>2</sub>-3h at 1 A g<sup>-1</sup>. (d) Long cycle performance of CM/TiO<sub>2</sub>-4h at 1 A g<sup>-1</sup>.

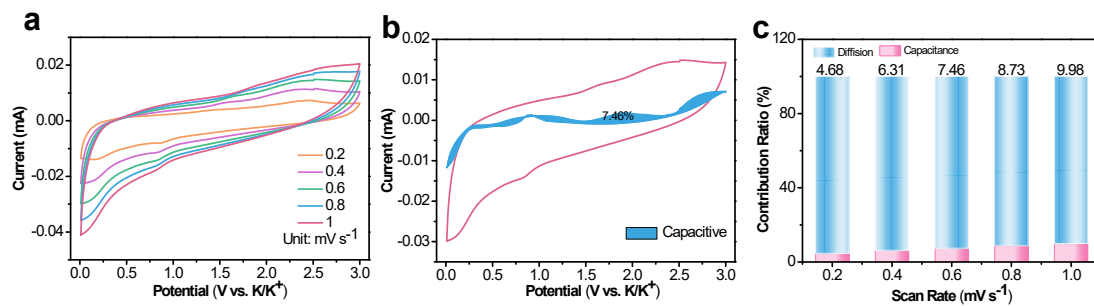


**Figure S9** (a) CV profiles of CM at different scan rates from 0.2 to 1.0 mV s<sup>-1</sup>. (b) Capacitive contribution of CM at 0.6 mV s<sup>-1</sup>. (c) Normalized contribution ratio of capacitive capacities in CM at various scan rates.

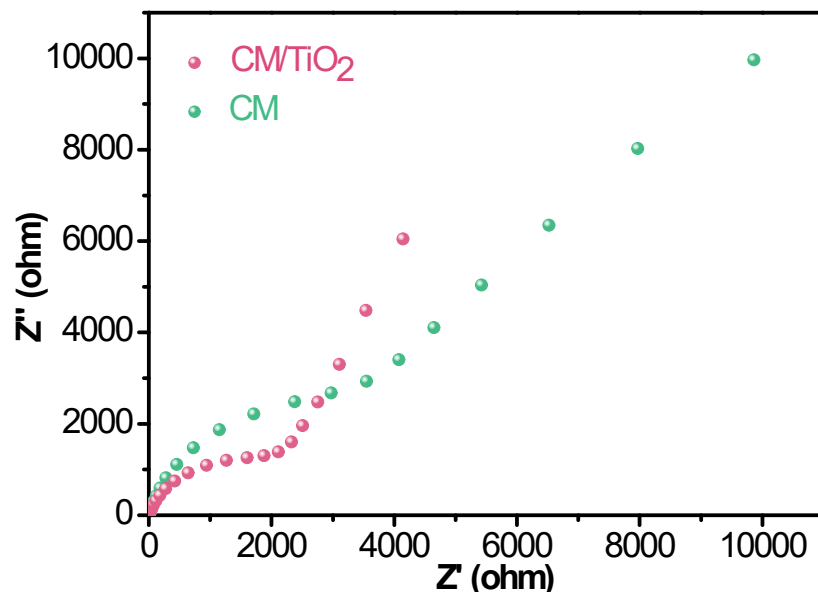


**Figure S10** Nyquist plot of CM/TiO<sub>2</sub> and CM after 100 cycles.

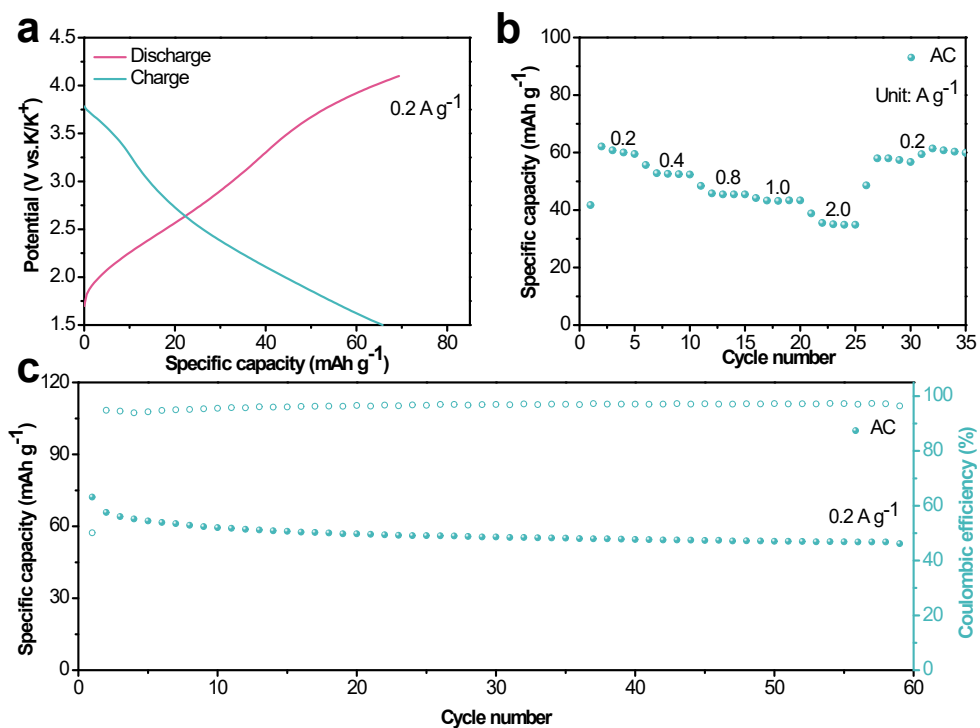


**Figure S11** (a) Galvanostatic charge/discharge curves of AC electrode at 0.2 A g<sup>-1</sup>. (b) Rate capability of AC electrode at various current densities. (c) Cycle performance of AC electrode at 0.2 A g<sup>-1</sup>.

**Table S1.** The comparisons of the reported anode for PIBs.

Electrodes	Low rate capacity	High rate capacity	Cycle number
<b>This work</b>	301 mA h g <sup>-1</sup> (0.1 A g <sup>-1</sup> )	94 mA h g <sup>-1</sup> (0.4 A g <sup>-1</sup> )	150 mA h g <sup>-1</sup> (0.05 A g <sup>-1</sup> , 100 cycles)
Ti <sub>3</sub> CN[1]	181 mA h g <sup>-1</sup> (0.02 A g <sup>-1</sup> )	80 mA h g <sup>-1</sup> (0.5 A g <sup>-1</sup> )	60 mA h g <sup>-1</sup> (0.1 A g <sup>-1</sup> , 100 cycles)
f-MXene[2]	119 mA h g <sup>-1</sup> (0.08 A g <sup>-1</sup> )	80 mA h g <sup>-1</sup> (0.5 A g <sup>-1</sup> )	120 mA h g <sup>-1</sup> (0.1 A g <sup>-1</sup> , 200 cycles)
a-Ti <sub>3</sub> C <sub>2</sub> T <sub>x</sub> [3]	167 mA h g <sup>-1</sup> (0.08 A g <sup>-1</sup> )	90 mA h g <sup>-1</sup> (0.2 A g <sup>-1</sup> )	50 mA h g <sup>-1</sup> (0.1 A g <sup>-1</sup> , 120 cycles)
Ti <sub>3</sub> C <sub>2</sub> [4]	119 mA h g <sup>-1</sup> (0.01 A g <sup>-1</sup> )	57 mA h g <sup>-1</sup> (0.5 A g <sup>-1</sup> )	30 mA h g <sup>-1</sup> (0.2 A g <sup>-1</sup> , 500 cycles)
h-MXene[2]	69 mA h g <sup>-1</sup> (0.08 A g <sup>-1</sup> )	39 mA h g <sup>-1</sup> (0.5 A g <sup>-1</sup> )	100 mA h g <sup>-1</sup> (0.1 A g <sup>-1</sup> , 200 cycles)
MXene Ti <sub>3</sub> C <sub>2</sub> [5]	105 mA h g <sup>-1</sup> (0.06 A g <sup>-1</sup> )	20 mA h g <sup>-1</sup> (0.5 A g <sup>-1</sup> )	80 mA h g <sup>-1</sup> (0.05 A g <sup>-1</sup> , 100 cycles)
N-UT-Ti <sub>3</sub> C <sub>2</sub> T <sub>x</sub> [6]	166 mA h g <sup>-1</sup> (0.09 A g <sup>-1</sup> )	141 mA h g <sup>-1</sup> (0.3 A g <sup>-1</sup> )	100 mA h g <sup>-1</sup> (0.1 A g <sup>-1</sup> , 100 cycles)

## Reference

- [1] J. Zhu, M. Wang, M. Lyu, Y. Jiao, A. Du, B. Luo, I. Gentle, L. Wang, Two-Dimensional Titanium Carbonitride MXene for High-Performance Sodium Ion Batteries, *ACS Applied Nano Materials* 1(12) (2018) 6854-6863.
- [2] P. Zhang, R.A. Soomro, Z. Guan, N. Sun, B. Xu, 3D carbon-coated MXene architectures with high and ultrafast lithium/sodium-ion storage, *Energy Storage Materials* 29 (2020) 163-171.
- [3] Yu Xie, Yohan Dall'Agnese, Michael Naguib, Yury Gogotsi, Michel W. Barsoum, Houlong L. Zhuang, and Paul R. C. Kent, Prediction and Characterization of MXene Nanosheet Anodes for Non-Lithium-Ion Batteries, *ACS Nano* (2014) 9606–9615.
- [4] P. Lian, Y. Dong, Z.-S. Wu, S. Zheng, X. Wang, W. Sen, C. Sun, J. Qin, X. Shi, X. Bao, Alkalized  $Ti_3C_2$  MXene nanoribbons with expanded interlayer spacing for high-capacity sodium and potassium ion batteries, *Nano Energy* 40 (2017) 1-8.
- [5] Z. Guo, G. Dong, M. Zhang, M. Gao, L. Shao, M. Chen, H. Liu, M. Ni, D. Cao, K. Zhu, Sulfur-Decorated  $Ti_3C_2T_x$  MXene for High-Performance Sodium/Potassium-Ion Batteries, *Chemistry – An Asian Journal* 18(18) (2023).
- [6] Y. Zhao, G. Dong, M. Zhang, D. Wang, Y. Chen, D. Cao, K. Zhu, G. Chen, Surface-engineered  $Ti_3C_2T_x$  MXene enabling rapid sodium/potassium ion storage, *2D Materials* 10(1) (2022).